

# Chain Selectivity of Tyrosine Contributions to Hemoglobin Static and Time-Resolved UVRR Spectra in $^{13}\text{C}$ Isotopic Hybrids

Daojing Wang, Xiaojie Zhao, and Thomas G. Spiro\*

Department of Chemistry, Princeton University, Princeton, New Jersey 08544

Received: July 15, 1999; In Final Form: September 8, 1999

Recombinant hemoglobin [Hb] has been labeled with  $^{13}\text{C}_6$ -tyrosine in order to characterize the tyrosine bands in static and time-resolved ultraviolet resonance Raman [UVRR] spectra. The large isotope shift for the Y8a/8b ring modes permits complete resolution of the important 1580–1660  $\text{cm}^{-1}$  region. Underlying bands from tryptophan [W1 and W17+18] and from phenylalanine [F8a] make only small contributions to static T–R and 150 ns time-resolved difference spectra. Isotopic hybrid Hb's were constructed in order to evaluate tyrosine contributions separately for  $\alpha$  and  $\beta$  chains. The Y8a and Y8b bands shift up significantly [2.5 and 3.2  $\text{cm}^{-1}$ ] in the  $\alpha$  but not the  $\beta$  chains for the T vs the R state. These shifts, along with an upshift of the Y9a band, are attributed to the T-state H-bonding of Tyr $\alpha$ 42, which is reinforced by a nearby positive charge. In the 150 ns time-resolved difference UVRR spectrum, both  $\alpha$  and  $\beta$  chains contribute to the negative tyrosine bands. These are suggested to arise from H-bond weakening of the penultimate residues, Tyr $\alpha$ 140 and  $\beta$ 145, as a result of F helix displacement in the initial [ $\text{R}_{\text{deoxy}}$ ] intermediate along the path from the R to the T states.

## Introduction

As part of a continuing effort to elucidate the allosteric reaction coordinate in hemoglobin [Hb],<sup>1–6</sup> we have examined the effect of  $^{13}\text{C}$  labeling of tyrosine residues on the static and time-resolved ultraviolet resonance Raman [UVRR] spectra. Laser excitation at 229 nm selectively enhances Raman bands arising from ring modes of tyrosine and tryptophan side chains.<sup>1,7,8</sup> These modes exhibit frequency and/or intensity changes when Hb undergoes the allosteric transition from the R to the T state as a result of deligation. The altered spectral bands reflect changes in the aromatic ring environments, principally in the nature and extent of hydrogen bonding. Thus, the tyrosine and tryptophan signals serve as structural reporters of the stages of the allosteric transition. Pump–probe techniques have been used to monitor these changes.<sup>1–3,6,9,10</sup>

However, structural interpretation of the UVRR signals is subject to ambiguities resulting from overlapping bands and from coincident signals of multiple residues having the same chemical composition. To help resolve these ambiguities, we have resorted to isotopic labeling of the tyrosine and tryptophan residues, by expressing recombinant Hb in *E. coli* auxotrophs grown in a medium containing labeled amino acids.<sup>11</sup> The isotope shifts of the tyrosine and tryptophan signals uncover bands that may be overlapped. In addition, the contributions of tyrosine and tryptophan residues on the different polypeptide chains,  $\alpha$  and  $\beta$ , can be disentangled by separating the labeled chains and combining them with unlabeled chains, to produce functional isotope hybrid Hb's. In this way, the multiple residue ambiguity is reduced, although not eliminated. The  $\beta$  chains have three tyrosine and two tryptophan residues, while the  $\alpha$  chains have three tyrosine and only one tryptophan residue.

We have previously reported results of labeling with Tyr- $d_4$  and Trp- $d_5$ .<sup>11</sup> Tryptophan contributions to the static T–R difference UVRR spectrum were almost completely resolved,

and important insights were obtained into the character of the tyrosine signals. However, interpretation of the tyrosine labeling results was hampered by the limited frequency shifts produced by the ring deuteration. To remove this limitation, we have now employed  $^{13}\text{C}_6$ -Tyr; incorporation of  $^{13}\text{C}$  at all six ring positions increases the frequency shifts for the important Y8a and Y8b modes (Figure 1). The new data permit complete characterization of these modes for  $\alpha$  and  $\beta$  chains and clarify the interpretation of chain-selective effects. We have also extended the isotope hybrid technique for the first time to time-resolved UVRR spectra, using a newly implemented frequency-quadrupled Ti:sapphire laser system.<sup>10</sup>

## Materials and Methods

**Recombinant Hemoglobin (rHb) Expression and Purification.** The recombinant human hemoglobin (rHb) was expressed from plasmid pHE2, in which synthetic human  $\alpha$ - and  $\beta$ -globin genes and the methionine aminopeptidase (Met-AP) gene from *E. coli* are coexpressed under the control of separate *tac* promoters.<sup>12</sup> The expression and purification of the natural-abundance rHb is described in detail elsewhere.<sup>11,13</sup> To efficiently incorporate  $^{13}\text{C}_6$ -Tyr into the protein, the plasmid was transformed into the host cell *E. coli* DL39 (DE3), which is auxotrophic for six amino acids: Tyr, Asp, Phe, Leu, Ile, and Val.<sup>14</sup> A defined M9 medium supplemented with 20 amino acids was used to produce the  $^{13}\text{C}_6$ -Tyr labeled rHb.  $^{13}\text{C}_6$ -Tyr was supplied at a minimal level for sufficient cell growth, which is about 25% of the concentration normally used in the defined medium.<sup>15</sup> Specifically, 1 L of medium contained 50 mg of L- $^{13}\text{C}_6$ -Tyr (98–99%, Cambridge Isotope Laboratories). The other procedures were the same as before.<sup>11</sup> The purity and homogeneity of the isotope-labeled rHb's were verified by polyacrylamide (10%) gel electrophoresis under both denaturing and nondenaturing conditions. Their identities were also confirmed by the electrospray mass spectroscopy (ESMS).

**Isotopic Hybrid Generation.** The  $\alpha$  and  $\beta$  chains of HbA and rHb were separated and assembled following standard

\* To whom correspondence should be addressed.

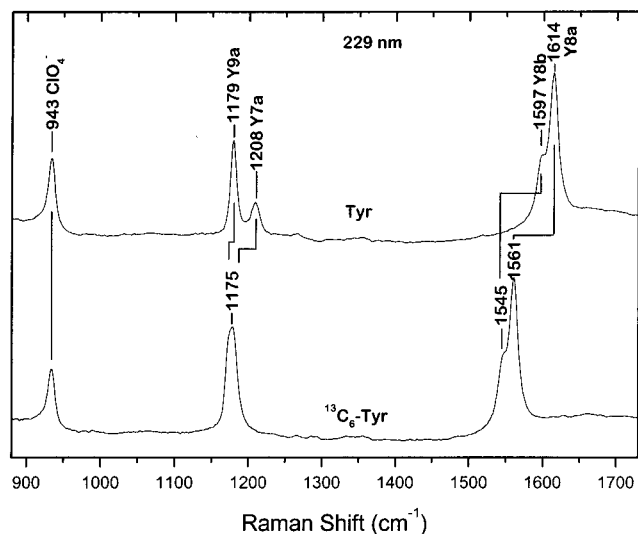


**Figure 1.** The 229 nm excited UVRR spectra of aqueous tyrosine and  $^{13}\text{C}_6$ -tyrosine (1 mM in 50 mM sodium phosphate, pH 7.4); 0.2 M  $\text{NaClO}_4$  was added as the frequency standard.

procedures.<sup>16</sup> The  $(\alpha^{13}\text{C})_2$  rHb was generated by reconstituting the isotope-labeled  $\alpha$  chain and natural-abundance  $\beta$  chain, and vice versa for  $(\alpha\beta^{13}\text{C})_2$  rHb.

**Static and Time-Resolved UVRR Spectroscopy.** The experimental setup has been described in detail elsewhere.<sup>1,10</sup> Protein samples were 0.4 mM in heme and exchanged into 50 mM sodium phosphate (pH 7.4), 0.5 mM EDTA. 0.2 M  $\text{NaClO}_4$  was used as the internal intensity standard to generate UVRR difference spectra.

**Determination of Frequency and Raman Cross Section of Tyr Bands in the UVRR Spectra.** Since isotope substitution in the tyrosine residues has no effect on the tryptophan spectrum, the strong W16 band was used as a secondary intensity standard when measuring tyrosine intensity differences between labeled and unlabeled samples in the same state. This procedure eliminated the influence of small concentration differences. These normalized spectra were used to generate the difference spectra in Figure 4. The Y8a/Y8b region (1580–1660  $\text{cm}^{-1}$ ) was then deconvoluted into two bands with 50% Gaussian and 50% Lorentzian shape. The Y7a band (1194–1229  $\text{cm}^{-1}$ ) was curve-fitted similarly. Raman cross sections were calculated based on the peak-heights. The cross section of  $\text{ClO}_4^-$  (0.586 mbarn molecule $^{-1}$  sr $^{-1}$ )<sup>17</sup> was employed to calculate the tyrosine cross sections from

$$\sigma_{\text{Tyr}} = (I_{\text{Tyr}}/I_{\text{ClO}_4^-})(C_{\text{ClO}_4^-}/C_{\text{Tyr}}) \sigma_{\text{ClO}_4^-}$$

## Results

**$^{13}\text{C}_6$ -Tyrosine Spectral Resolution.** The 229 nm-excited UVRR spectrum of tyrosine [Figure 1] contains bands arising from the ring modes Y8a [1614  $\text{cm}^{-1}$ ], Y8b [1597  $\text{cm}^{-1}$ ], Y7a [1208  $\text{cm}^{-1}$ ], and Y9a [1179  $\text{cm}^{-1}$ ].<sup>18</sup> In  $^{13}\text{C}_6$ -tyrosine, Y8a and Y8b shift down 53  $\text{cm}^{-1}$ , while Y7a and Y9a collapse to a single broad band, centered at 1175  $\text{cm}^{-1}$ .

These changes are apparent in the UVRR spectrum of  $^{13}\text{C}_6$ -tyrosine-labeled recombinant Hb [Figure 2]. The 1178  $\text{cm}^{-1}$  Y9a band is intensified and broadened, due to the shifted Y7a, and the Y8a and Y8b bands are shifted under the strong W3 band of the tryptophan residues. These shifts reveal underlying bands arising from tryptophan [W1, 1619  $\text{cm}^{-1}$ ; W17+W18, 1633  $\text{cm}^{-1}$ ] and phenylalanine [F8a, 1604  $\text{cm}^{-1}$ ; F7a, 1206  $\text{cm}^{-1}$ ].

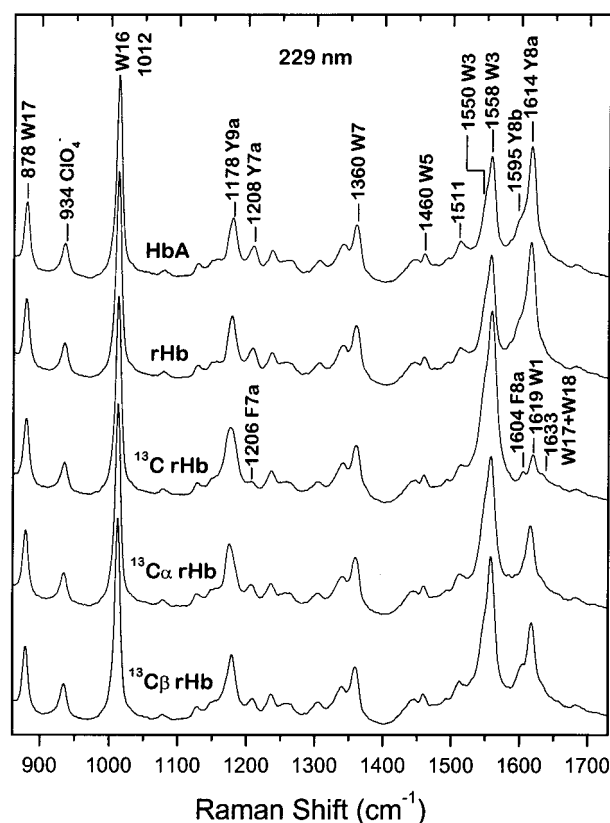


**Figure 2.** The 229 nm excited UVRR spectra of deoxy HbA, rHb,  $^{13}\text{C}_6$ -Tyr labeled rHb, and rHb labeled only in  $\alpha$  or  $\beta$  chains (pH 7.4, 0.4 mM in heme). (W = Trp modes, Y = Tyr modes, F = Phe modes). 0.2 M  $\text{NaClO}_4$  was used as the internal intensity standard. Separate positions are indicated for W3 from Trp $\beta$ 37 (1550  $\text{cm}^{-1}$ ) and Trp $\alpha$ 14/ $\beta$ 15 (1558  $\text{cm}^{-1}$ ).<sup>1,11</sup>

Despite Hb having 27 phenylalanine residues, their contribution to the UVRR spectrum is small because of low resonance enhancement at 229 nm.<sup>19</sup> As expected, the UVRR spectra of the isotopic hybrids are intermediate between those of unlabeled and fully labeled protein. Half the Y8a/8b intensity is shifted under the W3 band, and half the Y7a intensity is shifted under the Y9a band.

The effect of the T–R transition on the UVRR spectra of labeled Hb is seen in the deoxy Hb minus HbCO difference spectra [Figure 3]. The difference bands associated with tryptophan are the same in the fully labeled protein as in HbA or rHb, except that the W3 band is perturbed by the shifted Y8a/8b bands. This shift exposes the F8a, W1, and W17+W18 bands, whose contribution to the difference spectrum is seen to be detectable, but small. Their intensities are slightly higher in deoxyHb than in HbCO. The tyrosine difference bands for Y8a/8b and Y7a/9a are obscured in the labeled protein because of band overlaps.

**Chain-Selective T–R Signals.** The isotope hybrid difference spectra show clear differences between  $\alpha$  and  $\beta$  chains [Figure 3]. To interpret these differences, we subtracted the spectrum of fully labeled protein from the spectra of the hybrids and of HbA, thus canceling out all nontyrosine contributions. These isotope difference spectra [Figure 4] contain positive and negative bands for Y8a/8b and Y7a. There is also a slight negative band for Y9a, indicating an isotope effect on the intensity of this mode. The Y8a/8b and Y7a shifts are big enough to resolve the envelopes of the bands, thereby permitting direct comparison for the individual chains. Figure 5 shows this comparison for the Y8a/8b bands. It is evident that Y8a and Y8b are both at

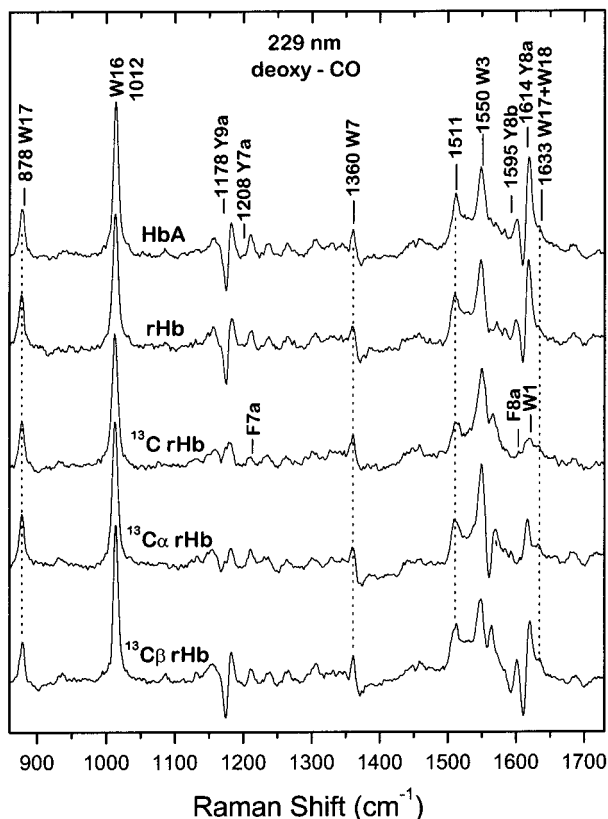


**Figure 3.** Same as Figure 2, but showing the UVRR difference spectra between deoxy and CO forms.

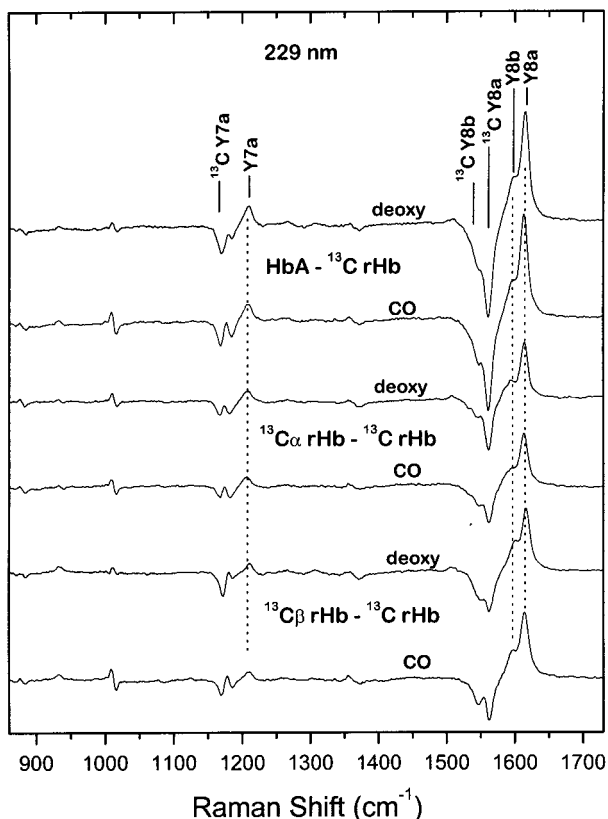


**Figure 4.** The 229 nm excited UVRR difference spectra between fully labeled rHb and HbA,  $\alpha$  chain labeled rHb and  $\beta$  chain labeled rHb, in both deoxy and CO forms.

higher frequencies in the  $\alpha$  than in the  $\beta$  chains for deoxy Hb, but not for HbCO.

These band envelopes were used to obtain chain-selective frequencies and intensities [Table 1] for the Y8a, Y8b and Y7a bands, using the curve-fitting procedures described in the materials and methods section. Corresponding values for HbA were obtained as a consistency check. The HbA parameters are averages of  $\alpha$  and  $\beta$  chain contributions. There are systematic differences between  $\alpha$  and  $\beta$  chains. Band frequencies are higher [ $1-5\text{ cm}^{-1}$ ] for the  $\alpha$  chains, as are the intensities. In addition, T-R differences are also chain-selective. Of particular significance are the different responses of Y8a and Y8b. In the  $\alpha$  chains, these bands shift up significantly in the T state, by 2.5 and  $3.2\text{ cm}^{-1}$ , respectively, while in the  $\beta$  chains, the shifts are much smaller,  $0.5$  and  $0.6\text{ cm}^{-1}$ . Intensities are higher in the T state, except that the Y8a intensity is essentially unchanged in the  $\alpha$  chains. This is why the Y8a T-R difference signal [Figure 3], shows a pure sigmoidal shape for the  $\alpha$  chains, reflecting the upshifted frequency, but a positive peak for the  $\beta$  chains, reflecting higher T state intensity with little frequency change [Figure 3].

The present results complement those reported previously for Hb hybrids which contain tyrosine- $d_4$ .<sup>11</sup> The same  $\alpha$ ,  $\beta$  chain distinction was found for Y8a, namely intensification for the  $\beta$  chains and a frequency upshift for the  $\alpha$  chains. However, the tyrosine- $d_4$  frequency shift was insufficient to resolve the Y8b band. The present data reveal an even larger T-state upshift for Y8b than for Y8a in the  $\alpha$  chains. On the other hand, the present data are uninformative about Y9a, whereas a large tyrosine- $d_4$  shift permitted the Y9a chain contributions to be distinguished.<sup>11</sup> Both chains showed comparable intensity losses in the T state but different frequency shifts. Y9a shifts up  $1.6\text{ cm}^{-1}$  in the  $\alpha$  chains, but down  $0.6\text{ cm}^{-1}$  in the  $\beta$  chains, between the R and the T states.<sup>11</sup> The frequency differences may explain why the Y9a T-R difference signal, which remains prominent when the  $\beta$  chain tyrosines are labeled with  $^{13}\text{C}$ , disappears when the  $\alpha$  chain tyrosines are labeled [Figure 3]. The loss in Y9a intensity in the T state is expected to cancel the gain in Y7a intensity [Table 1], when the latter is shifted into frequency coincidence with Y9a.

**Chain-Selective Time-Resolved Signals.** Time-resolved spectra were obtained at a 150 ns delay after HbCO photolysis in order to maximize formation of the first intermediate,  $R_{\text{deoxy}}$ , in the R-T transition.<sup>3,20</sup> The difference spectrum for this intermediate contains negative bands for tyrosine and tryptophan modes [Figure 6]. When all the tyrosines are labeled with  $^{13}\text{C}$ , the Y8a difference intensity shifts from 1614 to  $1561\text{ cm}^{-1}$ , where it overlaps with the W3 difference band. Also, the Y9a difference band is broadened, as a result of coincidence with the shifted Y7a band. The tryptophan W16 and W17 signals remain unaltered in the labeled protein. When the isotope hybrids are examined, the negative Y8a signals are seen to lose about half of their intensity, consistent with comparable contributions from  $\alpha$  and  $\beta$  chain tyrosines.

The bands in the 150 ns time-resolved spectra were quantified in the same way as the static spectra [Table 1]. The intensity losses were 10–30% for the Y8a, Y8b, and Y7a bands, with relatively small differences between  $\alpha$  and  $\beta$  chains. Slight frequency downshifts, relative to HbCO, were determined for Y7a and Y8b, but shifts were negligible for Y8a.

## Discussion

**T-R Signals.** The principal features of the T-R difference spectrum [Figure 3] are associated with the two important aromatic residue H-bonds across the  $\alpha_1\beta_2$  interface, namely Trp337...Asp $\alpha$ 94 and Tyr $\alpha$ 42...Asp $\beta$ 99.<sup>1</sup> These are formed in

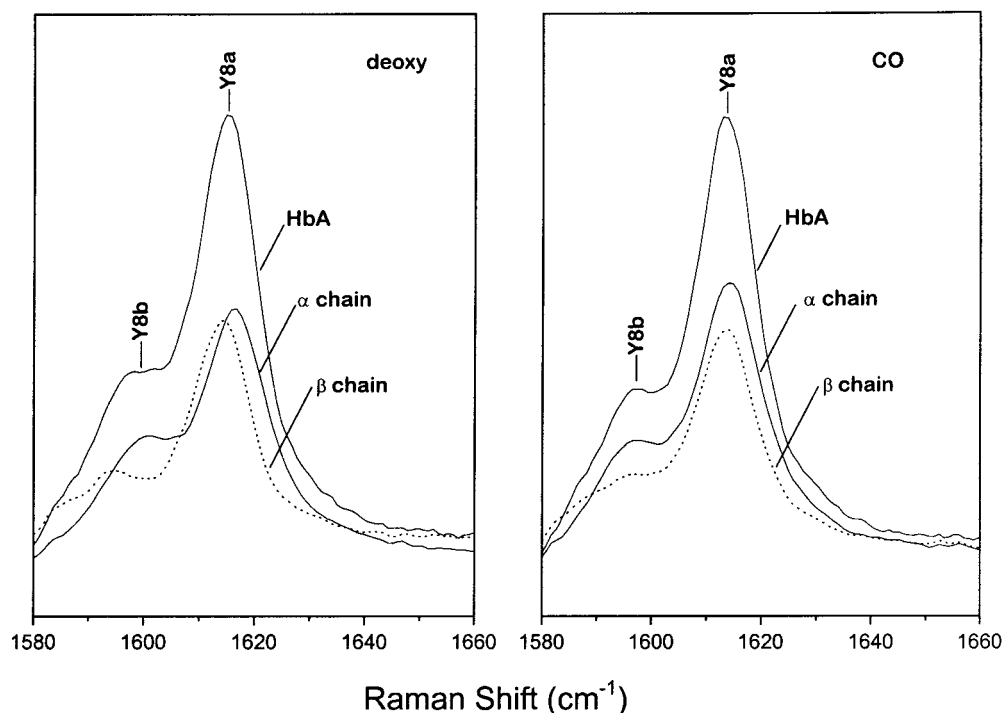


**Figure 5.** Expanded view of the Y8a/Y8b region in Figure 4, showing the pure tyrosine contribution in HbA and in the separate chains within the tetramer.

**TABLE 1: Frequency  $\nu$  ( $\text{cm}^{-1}$ ) and Raman Cross Section (peak height)  $\sigma$  ( $\text{mbarn molecule}^{-1} \text{sr}^{-1}$ ) of Tyr Y7a, Y8a, and Y8b Bands at pH 7.4**

		T	R	$\Delta_{\text{T/R}}$	150 ns	$\Delta_{\text{Rdeoxy/R}}$
HbA	$\nu_{8a}$	1615.1	1613.6	1.5	1613.6	0
	$\sigma_{8a}$	298	293	5	265	-28
	$\nu_{8b}$	1596.8	1595.0	1.8	1595.0	0
	$\sigma_{8b}$	98	73	25	62	-11
	$\nu_{7a}$	1208.9	1208.0	0.9	1207.8	-0.2
$\alpha$ chains	$\sigma_{7a}$	59	47	12	38	-9
	$\nu_{8a}$	1616.6	1614.1	2.5	1614.0	-0.1
	$\sigma_{8a}$	319	324	-5	292	-32
	$\nu_{8b}$	1598.6	1595.4	3.2	1595.3	-0.1
	$\sigma_{8b}$	124	99	25	89	-10
$\beta$ chains	$\nu_{7a}$	1210.8	1209.3	1.5	1208.7	-0.6
	$\sigma_{7a}$	63	52	11	42	-10
	$\nu_{8a}$	1614.0	1613.5	0.5	1613.2	-0.3
	$\sigma_{8a}$	285	269	16	245	-24
	$\nu_{8b}$	1593.6	1593.0	0.6	1592.7	-0.3
Tyr	$\sigma_{8b}$	80	57	23	44	-13
	$\nu_{7a}$	1207.1	1206.0	1.1	1205.7	-0.3
	$\sigma_{7a}$	60	48	12	38	-10
	$\nu_{8a}$	1614.2				
	$\sigma_{8a}$	284				

the T state and broken in the R state. Trp $\beta$ 37 has been shown via isotope labeling and mutagenesis to be responsible for most of the T-R difference scattering associated with tryptophan bands.<sup>1,11</sup>

In the case of tyrosine, the multiplicity of residues makes specific assignments less certain. The isotopic hybrid data make clear that the  $\alpha$  chains are responsible for the dominant T-R tyrosine difference signals, namely sigmoidal bands which reflect frequency shifts for Y8a, Y8b, and Y9a. Frequency shifts are substantial for the  $\alpha$  chains but small for the  $\beta$  chains [Table 1].<sup>7,11</sup> There are three tyrosine residues in the  $\alpha$  chains and three in the  $\beta$  chains. Table 2 lists the six residues and their H-bond

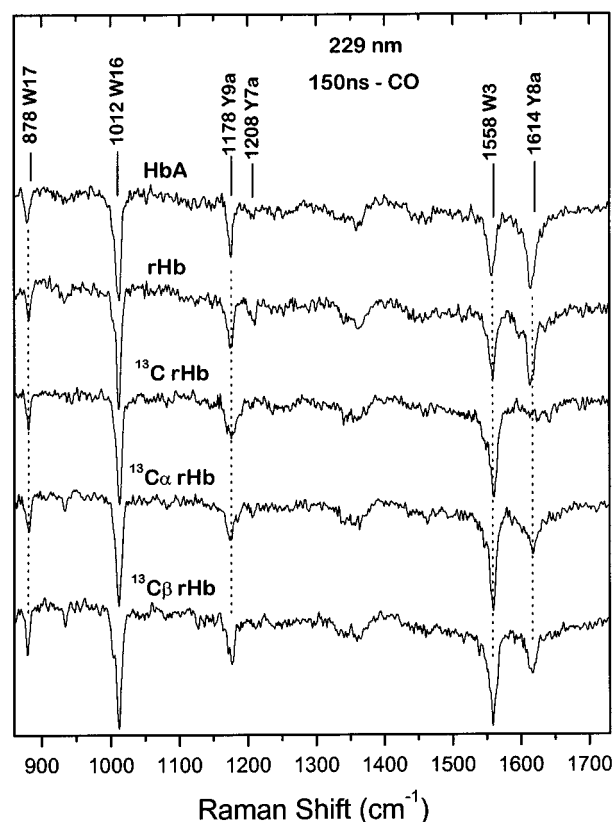


**Figure 6.** Pump-probe minus probe-pump UVRR difference spectra (pump = 419 nm, probe = 229 nm) at 150 ns time delay for CO forms of HbA, rHb, and isotope labeled species.

partners and O $\cdots$ O distances. Tyr $\alpha$ 24 has no H-bond partner, in either the T or the R state, and can therefore be discounted as a contributor to the UVRR difference spectrum. Tyr $\alpha$ 140 donates an intrachain H-bond to the Val $\alpha$ 93 carbonyl [Figure 7], but the crystal coordinates show the O $\cdots$ O distance to be

**TABLE 2: Tyr H-Bonding Parameters from HbA Crystallographic Coordinates<sup>a,b,c</sup>**

	deoxy HbA <sup>a,b</sup>		HbAO <sub>2</sub> <sup>c</sup>	
	partner	O...X (Å)	partner	O...X (Å)
Tyr $\alpha$ 24	none		none	
Tyr $\alpha$ 42	Asp $\beta$ 99	2.49/2.59	Water 49	2.85
Tyr $\alpha$ 140	Val $\alpha$ 93 (CO)	2.68/2.67	Val $\alpha$ 93 (CO)	2.67
			Val $\alpha$ 93 (NH)	2.79
Tyr $\beta$ 35	Asp $\alpha$ 126	3.33/3.09	Asp $\alpha$ 126	3.65
Tyr $\beta$ 130	Val $\beta$ 11	2.61/2.82	Val $\beta$ 11	2.51
Tyr $\beta$ 145	Val $\beta$ 98 (CO)	2.63/2.60	Val $\beta$ 98 (CO)	2.41
			Val $\beta$ 98 (NH)	2.91

<sup>a</sup> Deoxy HbA (1.74 Å; PDB, 2HHB).<sup>28</sup> <sup>b</sup> Deoxy HbA (1.8 Å; PDB, 1A3N).<sup>29</sup> <sup>c</sup> HbAO<sub>2</sub> (2.1 Å; PDB, 1HHO).<sup>30</sup>

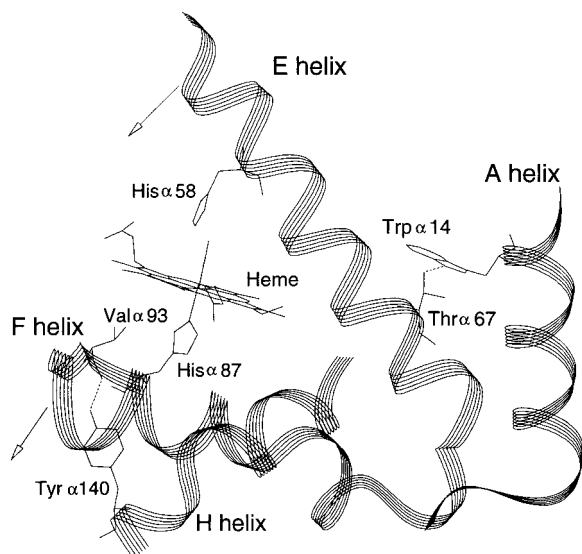


**Figure 7.** Diagram of the helix arrangement around the heme pocket of the  $\alpha$  chain of HbCO (PDB, 2HCO),<sup>31</sup> showing the H bond between Trp $\alpha$ 14 and Thr $\alpha$ 67, which bridges the A and E helices, and the H-bond between Val $\alpha$ 93 and Tyr $\alpha$ 140, which bridges the FG corner and the H helix. The arrangements are similar for  $\beta$  chains, except that Trp $\beta$ 15 and Ser $\beta$ 72 provide the A–E bridge, whereas Val $\beta$ 98 and Tyr $\beta$ 145 bridge the FG corner and H helix. Also shown are the heme and the proximal and distal histidine residues ( $\alpha$ 87 and  $\alpha$ 58). The arrows indicate the direction of E, F helix displacements after photodeligation as proposed in the model of the allosteric pathway.<sup>6</sup>

the same in the T and R states. Notwithstanding this result, Nagai et al.<sup>8</sup> proposed that the H-bond is weakened in the R state, because they found the Y8a and Y9a frequency shifts to be diminished when Tyr $\alpha$ 140 is mutated to histidine. However, this observation could equally well be attributed to an indirect effect of the mutation on the quaternary Tyr $\alpha$ 42...Asp $\beta$ 99 H-bond. Indeed the authors report a 3  $\text{cm}^{-1}$  upshift in the Fe–histidine stretching frequency, which is a sensitive indicator of T state constraints. They attributed this to reduced constraint on the proximal F helix as a result of the loss of the interhelical H-bond in the mutant. The reduced constraint could be communicated to Tyr $\alpha$ 42, loosening its H-bond.

Our view is that Tyr $\alpha$ 42 is responsible for the T–R frequency shifts, consistent with the results of mutating this residue. When Tyr $\alpha$ 42 is replaced by histidine<sup>8</sup> or by aspartate (with a compensating Asp $\beta$ 99Asn mutation),<sup>21</sup> the T–R difference UVR spectrum shows no frequency shift for Y8a, but only a slight intensification. However, the conundrum remains, as noted by Rodgers et al.,<sup>1</sup> that the frequency shifts are opposite to those expected for Tyr $\alpha$ 42. When tyrosine is a H-bond donor, the frequencies shift down, particularly for Y8b, which has been

calibrated for a series of H-bond acceptors.<sup>22</sup> The Y8b band is difficult to detect in UVR spectra of Hb, because it is a shoulder on the more intense Y8a, for which the frequency correlation with H-bonding is weaker.<sup>7,21</sup> However, a sigmoidal feature is consistently seen at the position of Y8b, as well as Y8a, in well-resolved T–R difference spectra [Figure 3]. A significant result of the present work is the determination of the Y8b upshift, which is 3.5  $\text{cm}^{-1}$  for the  $\alpha$  chains. The magnitude is significant, and the direction is clearly contrary to that expected for H-bond donation.<sup>22</sup>

To explain this contradiction we originally proposed<sup>1</sup> that Tyr $\alpha$ 42 was actually an acceptor of an H-bond from protonated Asp $\beta$ 99, but we subsequently disproved this hypothesis, since FTIR difference spectra of  $^{13}\text{C}$ -aspartate-labeled Hb were inconsistent with Asp protonation in the T state.<sup>23</sup> Instead, the expected Y8a/8b downshifts must be counterbalanced by compensating polarization of the Tyr $\alpha$ 42 side chain from H-bond donors or positive charges. In fact there is a H-bond donor to Tyr $\alpha$ 42, the backbone NH of Asp $\beta$ 94, and there is also a nearby positive charge, the side chain of Arg $\beta$ 40, whose guanidium C atom is 4.34 Å from the nearest ring atom of Tyr $\alpha$ 42 in the R state, but moves 0.5 Å closer in the T state.<sup>23</sup> This positive charge is probably the main cause of the anomalous Y8a,8b upshifts, and is of functional significance, since it re-enforces the Tyr $\alpha$ 42–Asp $\beta$ 99 H-bond, contributing to T state stabilization.

With respect to the  $\beta$  chain contributions to the T–R difference UVR spectrum, which are mainly intensity changes [Table 1],<sup>11</sup> the three  $\beta$  tyrosine residues all have H-bond partners and all show some change in O...O distance between the T and the R states [Table 2]. However, the O...O distances are quite long [3.1–3.6 Å] for Tyr $\beta$ 35, and Nagai et al.<sup>18</sup> have shown that replacing Tyr35 with phenylalanine or threonine has no detectable effect on the T–R difference spectra. Consequently, Tyr $\beta$ 35 can be ruled out as a contributor. In another experiment, Nagai et al. found that deletion of the C-terminal His $\beta$ 146 and Tyr $\beta$ 145 residues affected the T–R difference intensities of the tyrosine bands, and suggested a specific contribution from Tyr $\beta$ 145.<sup>8</sup> However, Wang and Spiro<sup>5</sup> have shown that the quaternary contacts are weakened in this construct, and are not fully restored by effectors [IHP, protons] that stabilize the T state. The Tyr $\beta$ 145 contribution cannot be separated from weakening of the Tyr $\alpha$ 42 quaternary H-bond. The third  $\beta$  chain tyrosine, Tyr $\beta$ 130, has not been investigated. It is H-bonded to the carbonyl of Val $\beta$ 11, providing a cross-link between the outermost helices, H and A.<sup>5</sup>) This H-bond is present in both the T and R states, and a small contraction of the O...O distance is indicated by the crystal coordinates [Table 2]. In summary, the  $\beta$  chain contributors to the tyrosine T–R difference signals must be Tyr $\beta$ 145 and/or Tyr $\beta$ 130, but the specific contributions are uncertain.

**R<sub>deoxy</sub> Signals.** The 150 ns time-resolved difference spectrum is associated with the initial protein structure change along the R–T reaction coordinate.<sup>2,3,5</sup> This spectrum contains only negative tyrosine and tryptophan bands [Figure 6]. It can be mimicked by subtracting the spectrum of tetraligated Hb from spectra of Hb constructs having one or more deligated chains within the R quaternary structure.<sup>2,5,24–26</sup> We have called this the R<sub>deoxy</sub> spectrum because it can be produced by removing one or more ligands from R-state Hb. Our hypothesis about the origin of this spectrum is that it arises from the weakening of aromatic residue H-bonds between the E and A helices, on one hand, and between the F and H helices on the other [Figure 7].<sup>2,6,13</sup> This weakening results from displacements of the E and

F helices upon deligation. When the Fe–ligand bond is broken, the Fe atom is displaced from the heme plane toward the proximal histidine ligand, which is attached to the F helix. The Fe displacement therefore exerts force on the F helix. On the distal side, departure of the ligand from the binding pocket permits displacement of the E helix toward the heme. The combination of Fe displacement and ligand loss is proposed to induce a rotation of the EF “clamshell”.<sup>6</sup> Such a rotation has recently been documented in high-resolution crystal structures of deoxy myoglobin and its CO adduct.<sup>27</sup> In myoglobin, the EF rotation angle is 1.7°, and backbone atoms in the vicinity of the proximal and distal residues are displaced by 0.3–0.4 Å. Displacements of this magnitude are sufficient to weaken H-bonds substantially.

We have recently employed site-directed mutagenesis to prove that the A–E interhelical H-bonds involving the Trp $\alpha$ 14 and Trp $\beta$ 15 residues are indeed weakened in the R<sub>deoxy</sub> intermediate.<sup>13</sup> The negative tryptophan bands in the 150 ns time-resolved difference spectrum are diminished when the H-bond acceptor residues are mutated. Thus, E helix displacement is strongly supported as part of the initial protein motion in response to deligation.

Important H–F interhelical H-bonds involve the penultimate tyrosine residues,  $\alpha$ 140 and  $\beta$ 145 as donors and the backbone carbonyls of the valine residues  $\alpha$ 93 and  $\beta$ 98 as acceptors.<sup>28–31</sup> Weakening of these H-bonds is expected to diminish the intensity arising from Tyr $\alpha$ 140 and  $\beta$ 145. Consistent with this expectation, the present results show that both  $\alpha$  and  $\beta$  chains contribute to the negative Y8a band in the time-resolved difference spectrum. The Y8b frequency shifts, although small, are also in the right direction for weakening of a donor H-bond [Table 1]. Thus, the isotope labeling experiment supports the EF clamshell rotation hypothesis. Site-directed mutagenesis experiments are in progress to establish the role of tyrosine H-bonding on the allosteric reaction path.

**Acknowledgment.** We thank Dr. Xuehua Hu for sharing his expertise in the protein expression. The ESMS measurements were performed in the electrospray mass spectrometry facilities at Princeton University (NIH IS10RRO). This work was supported by NIH Grant GM 25158 from the National Institute of General Medical Sciences.

## References and Notes

- (1) Rodgers, K. R.; Su, C.; Subramaniam, S.; Spiro, T. G. *J. Am. Chem. Soc.* **1992**, *114*, 3697.
- (2) Rodgers, K. R.; Spiro, T. G. *Science* **1994**, *265*, 1697.
- (3) Jayaraman, V.; Rodgers, K. R.; Mukerji, I.; Spiro, T. G. *Science* **1995**, *269*, 1843.
- (4) Hu, X.; Frei, H.; Spiro, T. G. *Biochemistry* **1996**, *35*, 13001.
- (5) Wang, D.; Spiro, T. G. *Biochemistry* **1998**, *37*, 9940.
- (6) Hu, X.; Rodgers, K. R.; Mukerji, I.; Spiro, T. G. *Biochemistry* **1999**, *38*, 3462.
- (7) Nagai, M.; Imai, K.; Kaminaka, S.; Mizutani, Y.; Kitagawa, T. *J. Mol. Struct.* **1996**, *379*, 65.
- (8) Nagai, M.; Wajcman, H.; Lahary, A.; Nakatsukasa, T.; Nagatomo, S.; Kitagawa, T. *Biochemistry* **1999**, *38*, 1243.
- (9) Kaminaka, S.; Ogura, T.; Kitagawa, T. *J. Am. Chem. Soc.* **1990**, *112*, 23.
- (10) Zhao, X.; Tengroth, C.; Chen, R.; Simpson, W. R.; Spiro, T. G. *J. Raman Spectrosc.*, in press.
- (11) Hu, X.; Spiro, T. G. *Biochemistry* **1997**, *36*, 15701.
- (12) Shen, T. J.; Ho, N. T.; Simplaceanu, V.; Zou, M.; Green, B. N.; Tam, M. F.; Ho, C. *Proc. Natl. Acad. Sci. U.S.A.* **1993**, *90*, 8108.
- (13) Wang, D.; Zhao, X.; Shen, T. J.; Ho, C.; Spiro, T. G. *J. Am. Chem. Soc.*, in press.
- (14) LaMaster, D. M.; Richards, F. M. *Biochemistry* **1988**, *27*, 142.
- (15) LaMaster, D. M.; Richards, F. M. *Biochemistry* **1985**, *24*, 7263.
- (16) Ikeda-Saito, M.; Inubushi, T.; Yonetani, T. *Methods Enzymol.* **1981**, *76*, 113.
- (17) Dudik, J. M.; Johnson, C. R.; Asher, S. A. *J. Chem. Phys.* **1985**, *82*, 1732.
- (18) Rava, R. P.; Spiro, T. G. *J. Phys. Chem.* **1985**, *89*, 1856.
- (19) Fodor, S. P. A.; Copeland, R. A.; Grygon, C. A.; Spiro, T. G. *J. Am. Chem. Soc.* **1989**, *111*, 5509.
- (20) Hofrichter, J.; Sommer, J. H.; Henry, E. R.; Eaton, W. A. *Proc. Natl. Acad. Sci. U.S.A.* **1983**, *80*, 2235.
- (21) Huang, S.; Peterson, E. S.; Ho, C.; Friedman, J. M. *Biochemistry* **1997**, *36*, 6197.
- (22) Hildebrandt, P. G.; Copeland, R. A.; Spiro, T. G. *Biochemistry* **1988**, *27*, 5426.
- (23) Hu, X.; Dick, L. A.; Spiro, T. G. *Biochemistry* **1998**, *37*, 9445.
- (24) Mukerji, I.; Spiro, T. G. *Biochemistry* **1994**, *33*, 13132.
- (25) Jayaraman, V.; Spiro, T. G. *Biochemistry* **1995**, *34*, 4511.
- (26) Huang, J.; Juszczak, J. L.; Peterson, E. S.; Vidugiris, G. V. A.; Friedman, J. M. *Biochemistry* **1999**, *8*, 4514.
- (27) Kachalova, G.; Popov, A. N.; Bartunik, H. D. *Science* **1999**, *284*, 473.
- (28) Fermi, G.; Perutz, M. F.; Shaanan, B.; Fourme, R. *J. Mol. Biol.* **1984**, *175*, 159.
- (29) Tame, J.; Vallone, B. Protein Data Bank, 1A3N; 1998.
- (30) Shaanan, B. *J. Mol. Biol.* **1983**, *171*, 31.
- (31) Baldwin, J. M. *J. Mol. Biol.* **1980**, *136*, 103.